Atmos. Meas. Tech. Discuss., doi:10.5194/amt-2016-276, 2016
Manuscript under review for journal Atmos. Meas. Tech.
Published: 16 November 2016
© Author(s) 2016. CC-BY 3.0 License.

Atmospheric Measurement Techniques Discussions

Estimation and Evaluation of COSMIC Radio Occultation Excess Phase Using Non-differenced Measurements

Pengfei Xia*, Shirong Ye*✉, Kecai Jiang, Dezhong, Chen
GNSS Research Centre, Wuhan University, Wu han, 430079,China
Correspondence to: *Ye Shirong (srye@whu.edu.cn)*

Abstract. In the GPS radio occultation technique, the atmospheric excess phase (AEP) can be used to derive the refractivity which is an important quantity in numerical weather prediction. The AEP is conventionally estimated based on GPS double-differenced or single-differenced techniques. These two techniques, however, require the reference link data in the data processing increasing the complexity of computation. In this study, a non-differenced (ND) processing strategy is proposed to estimate the AEP. To begin with, we used PANDA (Positioning and Navigation Data Analyst) software to perform the precise orbit determination (POD) for the COSIMC (The Constellation Observing System for Meteorology, Ionosphere and Climate) satellite to acquire the position and velocity of the center of mass of the satellite and the corresponded receive clock offset. The bending angles, refractivity and dry temperature profiles are derived from the estimated AEP by the ROPP (Radio Occultation Processing Package) software. The ND method is validated by the COSMIC products in typical rising and setting occultation events. Comparison results indicate that RMS (root mean square) errors of relative refractivity differences between ND-derived and "atmPrf" profiles are better than 4% and 3% in rising and setting occultation events, respectively. In addition, we also compared the relative refractivity bias between ND-derived and "atmPrf" profiles of globally distributed 200 COSMIC occultation events on December 12, 2013. The statistic results show that the average RMS relative refractivity deviation between ND-derived and COSMIC profile is better than 2% in the rising occultation event, and it is better than 1.7% in setting occultation event. Moreover, the observed COSMIC refractivity profiles from ND processing strategy are further validated using European Centre for Medium-Range Weather Forecasts (ECMWF) analyses data, and the results indicate that non-differencing reduces the noise level on the excess phase paths in the lower troposphere compared to single difference processing strategy.

Keywords: Radio Occultation; Excess Phase; Precise Orbit Determination; GPS

1. Introduction

Atmos. Meas. Tech. Discuss., doi:10.5194/amt-2016-276, 2016
Manuscript under review for journal Atmos. Meas. Tech.
Published: 16 November 2016
© Author(s) 2016. CC-BY 3.0 License.

Atmospheric Measurement Techniques Discussions

The radio occultation (RO) technique was first applied in the field of astronomy for detecting the state of the planet's atmosphere (Kursinski et al., 1997). With the development of GPS meteorology, the space-based GPS radio occultation is regarded as a valuable data source for atmospheric change studies (Rocken et al., 1997; Kursinski et al., 1997; Hajj et al., 2002; Beyerle et al., 2005). Since the GPS/MET (Global Positioning system/Meteorology) mission conducted a number of successful measurement experiments from 1995 to 1997 (Ware et al., 1996; Rocken et al., 1997), some low Earth orbiting (LEO) satellites, such as: CHAMP, GRACE, COSMIC and MetOp-A (Wickert et al., 2001, 2005; Rocken et al., 2000; Wilson et al., 2010), have begun to equip RO instruments facilitating the development of RO technique. In the GPS occultation technique, the atmospheric refractivity is an important quantity in the numerical weather prediction (Esteban et al., 2013). The atmospheric excess phase (AEP) can be used to derive the bending angles of the GPS rays and further to obtain the refractivity from the bending angles. Thus, the retrieval accuracy of refractivity is quite dependent on the quality of the estimated AEP.

Conventionally, the AEP is determined using two kinds of differential technique, i.e. double-difference (DD) (Sokolovskiy et al., 1996; Kursinski et al., 1997; Rocken et al., 1997; Hajj et al. 2002) and single-difference (SD) (Wickert et al., 2002; Schreiner et al., 2005), in which various errors can be eliminated from the differencing of GPS observations. The double-differenced method requires additional data from the ground receiver and the reference GPS satellite to remove the oscillator errors of the transmitter and the LEO receiver. This processing will bring the error sources to AEP from the ground data and the reference GPS satellite, such as multipath error, residual ionospheric and troposphere noise, thermal noise, and so on (Schreiner et al., 2010). Single-difference processing has a potential advantage over double-differencing since it can eliminate the ground observation data error (Schreiner et al., 2010). However, single-difference excess phases also suffer the noise sources from the reference link data. Compared with the two differential techniques, non-differenced (ND) method does not require the reference link data, which reduces the complexity in data processing. Besides, ND processing can potentially obtain lower noise AEP by utilizing prior estimated LEO and GPS clocks (Beyerle et al., 2005; Schreiner et al., 2011). Beyerle et al (2005) firstly proposed the idea of ND technique to estimate the AEP, and successfully analyzed the GRACE-B satellite to correct the effect of receiver clock by

Atmos. Meas. Tech. Discuss., doi:10.5194/amt-2016-276, 2016
Manuscript under review for journal Atmos. Meas. Tech.
Published: 16 November 2016
© Author(s) 2016. CC-BY 3.0 License.

Atmospheric Measurement Techniques Discussions

interpolating the temporal resolution of 30s GRACE-B's receiver clock solutions into 20 ms. Their results show that there is a good agreement of the refractivity between ND-derived and SD-derived in the upper troposphere and lower stratosphere. More significantly, ND technique can reduce the noise level and yield less-biased refractivity in the lower troposphere compared to SD technique. However, ND technique needs a LEO receiver with an ultra-stable oscillator (Beyerle et al. 2005; Schreiner et al., 2010). Therefore, "single difference" method is still widely utilized to get AEP in the current international various GPS RO data processing centers (Bi et al., 2012).

The accuracy of ND-derived refractivity mainly depends on the quality of clock error. COSMIC (The Constellation Observing System for Meteorology, Ionosphere and Climate) satellites' orbits and clock solutions are provided at a temporal resolution of 30s. Subject to the effect of COSMIC receiver oscillator, a lot of noises will be introduced when interpolating 30s clock solutions into 20 ms. In this study, we adopt PANDA (Positioning And Navigation Data Analyst) software to determine the COSMIC satellite orbit and obtain the receiver clock error at an interval of 1s. Then, the AEP is extracted utilizing the ND technique. Additionally, the refractivity and dry temperature will be derived from the AEP based on ROPP (Radio Occultation Processing Package) software. Finally, we compared the ND-derived refractive with the "atmPrf" profiles provided by UCAR/CDAAC (University Corporation for Atmospheric Research/COSMIC Data Analysis and Archive Center). Moreover, the ND-derived refractivity profiles were further evaluated by comparing with the analyze field data of ECMWF (European Centre for Medium-Range Weather Forecasts).

The rest of the paper is organized as follows. Section 2 introduces the principle of estimating AEP using non-difference method. Section3 describes the processing of LEO precise orbit determination using PANDA software. Section 4 presents the validation of ND-derived refractivity. The conclusions are included in Section5.

2 Non-Differencing Method

The signals of the GPS occulting satellite are recorded by the RO receiver aboard the spacecraft in 50 Hz during the occultation event. The carrier phase measurements with repaired cycle slip can be expressed as (Schreiner et al., 2010):

Atmos. Meas. Tech. Discuss., doi:10.5194/amt-2016-276, 2016
Manuscript under review for journal Atmos. Meas. Tech.
Published: 16 November 2016
© Author(s) 2016. CC-BY 3.0 License.

Atmospheric Measurement Techniques Discussions

$$Li_r^s(t_r) = c \cdot \delta t_r(t_r) + c \cdot \delta t_{r,rel}(t_r) + \rho_r^s(t_r) + \rho_{r,rel}^s(t_r) + c \cdot \delta t^s(t_r - \tau_r^s) + c \cdot \delta t_{rel}(t_r - \tau_r^s) + \delta\rho_{r,\mathrm{ion}}^s(t_r) + \delta\rho_{r,trop}^s(t_r) + \lambda_i \cdot N_{amb} + V_{\mathrm{pco}} + \varepsilon \quad (1)$$

where i=1,2; t_r and δt_r indicate the receive time and the deviation between receiver time and right time at receive time, respectively; c is the speed of light in vacuum; $\delta t_{r,rel}$ represents the offset between right time and coordinate time at the receiver owing to special and general relativity; t^s and δt^s denote the transmitted time and the deviation between proper time and satellite time at transmit time, respectively; δt^s_{rel} expresses the offset between right time and coordinate time at satellite; ρ^s_r is the geometric range between GPS satellite and COSMIC satellite; $\delta\rho^s_{r,rel}$ means gravitational delay correction; $\delta\rho^s_{r,ion}$ and $\delta\rho^s_{r,trop}$ signify the ionospheric delay correction and tropospheric delay correction, respectively; τ^s_t indicates the light travel time in vacuum; N_{amb} represent phase ambiguity; V_{pco} means the antenna phase center offsets; ε is phase noise.

The above equation neglects multipath errors, carrier phase wind-up and so on. The position and the clock error of GPS satellite are provided by the International GNSS Service (IGS). In addition, the τ^s_t, δt^s_{rel} and $\delta\rho^s_{r,rel}$ can be modeled utilizing the following equations (Schreiner et al., 2010):

$$\tau_r^s = \frac{\left(\rho_r^s(t_r) + \delta\rho_{r,\mathrm{rel}}^s\right)}{c} \quad (2)$$

$$\delta t_{rel}^s = -2\frac{r^s \cdot v^s}{c^2} \quad (3)$$

$$\delta\rho_{r,rel}^s = \frac{2GM_E}{c^2}\ln\left(\frac{r^s + r_r + \rho_r^s}{r^s + r_r - \rho_r^s}\right) \quad (4)$$

where r^s and r_r mean the position and velocity vectors of the GPS satellite at signal transmit time in an earth-centered inertial (ECI) reference frame (Ashby 2003); G denotes Newton's gravitational constant; M_E expresses the earth's mass; r^s and r_r represent the GPS satellite and receiver radial positions at the GPS signal transmit and receive times.

The *L1* and *L2* channel phase can be combined with satellite position and velocity data to determine the AEP. Neglecting the influences of ambiguity and time-independent error terms, the use of ND method to calculate the AEP (ΔL_i) can be modeled as follows (Schreiner et al., 2010):

$$\Delta L_i = \delta\rho_{r,\mathrm{ion}}^s(t_r) + \delta\rho_{r,trop}^s(t_r) = Li_r^s(t_r) - c \cdot \delta t_r(t_r) - c \cdot \delta t_{r,rel}(t_r) - \rho_r^s(t_r) - \rho_{r,rel}^s(t_r) - c \cdot \delta t^s(t_r - \tau_r^s) - c \cdot \delta t_{rel}(t_r - \tau_r^s) - V_{pco} \quad (5)$$

The input *L1* and *L2* phase measures of COSMIC RO are provided by the "opnGps" profiles

Atmos. Meas. Tech. Discuss., doi:10.5194/amt-2016-276, 2016
Manuscript under review for journal Atmos. Meas. Tech.
Published: 16 November 2016
© Author(s) 2016. CC-BY 3.0 License.

which can be downloaded in UCAR/CDAAC at a temporal resolution of 20 ms. Besides, UCAR/CDAAC also supply the COSMIC receiver clock offset "leoClk" profile and the GPS satellite clock offset "comClk" profile at a temporal resolution of 30 s. Each of the COSMIC satellites is equipped with the BlackJack GPS receiver, a tiny ionospheric photometer (TIP) and a tri-band beacon (TBB) (Wu et al. 2005; Schreiner 2005; Montenbruck et al. 2006), and the Integrated GPS Occultation Receiver (IGOR) is designed by the Jet Propulsion Laboratory (JPL) and manufactured by Broad Reach Engineering (Schreiner et al. 2011). By analyzing the results of "leoClk" profiles, we conclude that the turbulence of IGOR receiver clock is relatively serious. Therefore, estimated AEP at the required temporal resolution of 20 ms could not be interpolated successfully from the 30 s clock solutions utilizing Eqs.(5). It will be an effective technique to deal with this problem by reprocessing the COSMIC satellite orbit and obtaining the high accurate and high temporal resolution of IGOR clock offset.

3 COSMIC spacecraft precise orbit determination

3.1 COSMIC POD processing

The joint Taiwan/US mission COSMIC, including six micro-satellites, was launched on April 17, 2006. Each of the satellites is equipped with a GPS receiver which is installed with four antennas on the front and back faces of the satellite main frame. Two single-patch antennas, mounted on the upper part of the main body, are for POD. The other two antennas, dedicated to atmospheric occultation research, are mounted on the lower part (Hwang et al., 2009). The POD of COSMIC satellite is an important premise in atmospheric occultation research. At present, UCAR (University Corporation for Atmospheric Research) provides three kinds of COSMIC orbit products, i.e. reprocessing products, post-products and real-time products. UCAR/CDAAC reprocess products adopt Bernese5.2 software as processing tool, and orbit determination method is improved as well as the processing method of the phase values is more elaborate. The three-dimensional position average RMS value of overlapping orbit precision is superior to 15 cm, and the three-dimensional velocity RMS value is better than 0.15 mm/s (CDAAC, 2013). In addition, Hwang et al., (2009) calculated the COSMIC satellite orbits using Bernese 5.0 software and differences between their orbit products and those of UCAR are at the level of 10 cm on three axis.

Atmos. Meas. Tech. Discuss., doi:10.5194/amt-2016-276, 2016
Manuscript under review for journal Atmos. Meas. Tech.
Published: 16 November 2016
© Author(s) 2016. CC-BY 3.0 License.

Atmospheric Measurement Techniques Discussions

PANDA is satellite positioning and orbit determination software which is an independent research and development product by satellite navigation and positioning technology research center of Wuhan University. The software has the ability of processing many kinds of observation data, such as GNSS (including GPS, GLONASS, GALILEO, and BDS), SLR, KBR, satellite attitude and so on (Liu et al., 2004). In the paper, the PANDA software is exploited to perform POD for the COSMIC satellite. The process of this inputs include the COSMIC L1 and L2 pseudo-range and carrier phase data form the HAICH-FARR antenna, COD Final GPS orbits, 5-s COD-provided transmitter clock offsets from GPS time, LEO attitude information from CDAAC, earth orientation information and L1and L2 antenna phase center variations. Ionosphere-free phase observations are utilized based on a post-processing generalized least squares approach to determine the position and velocity of the center of mass of the LEO satellite as a function of coordinate time in an ECI reference frame and clock of the LEO every 1 second. In the process, the POD is calculated over 30-hour data arcs utilizing 1Hz carrier phase observations from HAICH-FARR antenna. The state vector computed in this processing also take the influence of dynamic model or estimation method into account, such as the gravitational field, the earth and ocean tides, tidal dynamic model, solar radiation pressure, experience force and so on. Furthermore, gravity field uses EIGEN2 model whose order is set to 140, and solar radiation pressure uses box-wing model.

3.2 POD Precision Evaluation

In the processing of POD, firstly we can obtain the initial COSMIC satellite orbit, state parameters and mechanical parameters through the pseudo-range single point positioning, then such initial solutions can be used for orbit integration in order to achieve the purpose of further elaboration. The next stage of processing is to detect gross errors and cycle slips of the GPS carrier phase data, then the COMSIC orbit precision will be improved according to the residual errors to iterative least squares estimate and residual edit operation. Finally, the orbit and clock error will be output every second. In order to test the accuracy of COSMIC orbits from PANDA software, we selected 53-day satellite-borne GPS observation data from day of year (DOY) 313 to 365 of 2011which is provided by UCAR/CDAAC. Due to the missing of 3th COSMIC satellite data, we only processed

Atmos. Meas. Tech. Discuss., doi:10.5194/amt-2016-276, 2016
Manuscript under review for journal Atmos. Meas. Tech.
Published: 16 November 2016
© Author(s) 2016. CC-BY 3.0 License.

Atmospheric Measurement Techniques Discussions

the remaining 5 satellites' data and removed those data with observation time less than 10 hours. Since the COSMIC satellites are not equipped with laser corner reflector, the accuracy of orbit determination cannot be evaluated by SLR precision ranging information. We thus mainly compared our orbit results with UCAR/CDAAC to analyze the precision of orbit determination. The statistical results of five satellites orbit between PANDA-derived and UCAR/CDAAC-derived are given in Table 1. In addition, there is a 6-hour overlapping orbit between the tracks because of the usage of 30 hours data arcs as the orbit determination length. Table 2 presents the RMS of COSMIC satellites which are compared with overlapping orbits on three axis direction.

Table 1. The RMS of COSMIC satellites compared with UCAR/CDAAC on three axis direction

	Radial RMS		Along-track RMS		Cross-track RMS		3-D Root Sum Square	
	Pos (cm)	Vel (mm/s)	Pos (cm)	Vel (mm/s)	Pos (cm)	Vel (mm/s)	Pos (cm)	Vel (mm/s)
FM1	10.82	0.117	13.29	0.115	13.91	0.134	22.07	0.212
FM2	10.40	0.162	16.99	0.105	9.65	0.097	22.13	0.216
FM4	7.92	0.103	12.38	0.085	11.70	0.120	18.78	0.180
FM5	8.89	0.123	14.39	0.097	12.48	0.087	21.01	0.179
FM6	10.06	0.139	16.28	0.109	10.63	0.094	21.89	0.200

Table 2. The RMS of COSMIC satellites compared with overlapping orbits on three axis direction

	Radial RMS		Along-track RMS		Cross-track RMS		3-D Root Sum Square	
	Pos (cm)	Vel (mm/s)	Pos (cm)	Vel (mm/s)	Pos (cm)	Vel (mm/s)	Pos (cm)	Vel (mm/s)
FM1	5.37	0.051	6.57	0.058	6.67	0.048	10.80	0.091
FM2	5.30	0.058	6.55	0.054	5.63	0.049	10.13	0.093
FM4	6.11	0.079	8.09	0.058	6.30	0.056	11.93	0.113
FM5	4.94	0.069	8.07	0.053	7.02	0.057	11.78	0.105
FM6	6.91	0.079	8.58	0.077	7.35	0.057	13.25	0.124

As shown in Table 1, the average 3-D RMS orbit coordinates and velocity differences between PANDA-derived and UCAR/CDAAC-derived for the 53-day period are 11.98 cm and 0.11 mm・s^{-1}, respectively. In addition, Table 1 presents that the accuracy of 4th COSMIC satellite's POD is better than the other four satellites. Table 2 shows the average 3-D RMS POD's coordinates and velocity are better than 6.63 cm and 0.06 mm·s^{-1} compared with overlapping orbits and velocity, respectively. These results suggest that the quality of COSMIC POD generated from PANDA software is feasibly.

4 Results validation and analysis

Atmos. Meas. Tech. Discuss., doi:10.5194/amt-2016-276, 2016
Manuscript under review for journal Atmos. Meas. Tech.
Published: 16 November 2016
© Author(s) 2016. CC-BY 3.0 License.

Atmospheric Measurement Techniques Discussions

The UCAR COSMIC Data Analysis and Archive Center data processing center adopted the method of single-difference to process data of COSMIC radio occultation, meanwhile deposited the processed excess phase delay into "atmPhs" profile. Atmospheric profiles of bending angle, refractivity and dry temperature generated from "atmPhs" files were written into "atmPrf" profiles. These files are freely available for public access http://cdaac-www.cosmic.ucar.edu/. In order to evaluate the precision of AEP estimated by ND method, the AEPs are obtained using Eqs.(5) in this study. Then, the ROPP software is implemented to process excess phase data and deriving profiles of bending angle, dry temperature and refractivity. Finally, the obtained COSMIC refractivity profiles are compared with "atmPrf" profiles provided by UCAR/CDAAC. Furthermore, duo to UCAR/CDAAC also offers the moisture profiles generated from ECMWF analysis and the ERA (Each re-analysis) interim model which collocated with occultation profiles. So the comparison between ND-derived refractivity and meteorological analysis results are performed to further validate the results obtained from ND method.

4.1 The results of typical GPS occultation event

Non-differenced processing strategy is utilized to obtain L1 and L2 excess atmospheric phases as functions of GPS time in an ECI TOD (true equator and equinox of data) reference frame. Inputs to this processing are: 50Hz L1 and L2 phase measures for the occulting GPS satellite, LEO and GPS positions, velocities and clock offsets, and antenna phase center information. Then, the AEPs are calculated using Eqs.(5), randomly selecting two GPS occultation events on December 12, 2013. Table 3 gives the detailed status parameters of the two GPS occultation events.

Table 3. Detailed status parameters of the selected two GPS occultation events on December 12, 2013

Parameter	OCCsat-1	OCCsat-2
GPS	PRN-08	PRN-28
LEO	CO06	CO05
start time	15:07	14:12
last time	123s	146s
status	setting	rising
longitude	3.78˚E	-109.84˚W
latitude	34.06˚N	26.08˚N
quality mark	bad=0	bad=0

As the method introduced by section 2, we first process the two GPS occultation events to obtain AEPs by ND technique. Afterwards, these atmospheric excess phases and collocated with occultation "atmPhs" profiles will be used for generating refractivity based on ROPP software,

Atmos. Meas. Tech. Discuss., doi:10.5194/amt-2016-276, 2016
Manuscript under review for journal Atmos. Meas. Tech.
Published: 16 November 2016
© Author(s) 2016. CC-BY 3.0 License.

Atmospheric Measurement Techniques Discussions

216 respectively. We named them as Ref_ND and Ref_Phs, respectively. Using the "atmPrf" profiles
217 of refractivity provided by UACR/CDAAC as references, ROPP software is validated by
218 comparing Ref_Phs with atmPrf products. Moreover, the Ref_ND is evaluated by comparing with
219 Ref_Phs and atmPrf products, respectively. These results are depicted by Figure 1 and Figure 2.

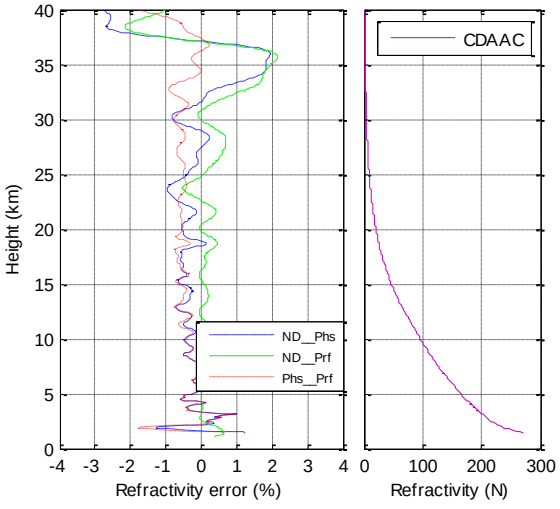

220
221 **Fig. 1.** The results of ND_Phs, ND_Prf and Phs_Prf in the setting radio occultation. ND_Phs expresses the relative
222 refractivity offset between Ref_ND and Ref_Phs; ND_Prf denotes the relative refractivity offset between Ref_ND
223 and "atmPrf"; Phs_Prf indicates the relative refractivity offset between Ref_Phs and "atmPrf" product; Ref_ND
224 means the refractivity obtained from ND-derived AEP based on ROPP software; Ref_Phs means the refractivity
225 obtained from atmPhs profiles based on ROPP software.
226

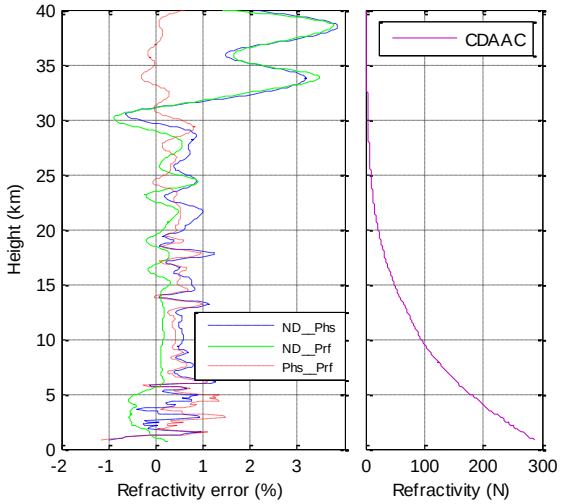

227
228 **Fig. 2.** The results of ND_Phs, ND_Prf and Phs_Prf in the rising radio occultation. ND_Phs expresses the relative

Atmos. Meas. Tech. Discuss., doi:10.5194/amt-2016-276, 2016
Manuscript under review for journal Atmos. Meas. Tech.
Published: 16 November 2016
© Author(s) 2016. CC-BY 3.0 License.

Atmospheric Measurement Techniques Discussions

refractivity offset between Ref_ND and Ref_Phs; ND_Prf denotes the relative refractivity offset between Ref_ND and "atmPrf"; Phs_Prf indicates the relative refractivity offset between Ref_Phs and "atmPrf" product; Ref_ND means the refractivity obtained from ND-derived AEP based on ROPP software; Ref_Phs means the refractivity obtained from atmPhs profiles based on ROPP software.

Figure 1 and Figure 2 show the results for the setting and rising occultation, respectively. The red dashed lines are less than ±1.7% under the height of 40m, which verifies the feasibility of ROPP software. In addition, the green lines are closer to 0 than red lines and blue lines under the height of 30km while the green line and blue line are gradually increases from the height of 30km to 40km. Besides, Figure 1 and Figure2 also depict that the refractivity is exponential change with height, and the refractivity is less than 5N from the height of 30km to 40km.

4.2 The statistic and verified of ND method

The COSMIC RO provides about 1800 RO events per day and the science mission is mainly for weather, climate, space weather, geodetic research and so on study purpose (Yen et al., 2007; Kuo et al., 2007). To verify the ND method, we randomly selected 200 RO events on December 12, 2013 to obtain the AEP utilizing Eqs.(5), then deriving profiles of refractivity and dry temperature through ROPP software which are named R_N and T_N, respectively. Figure 3 shows the distribution of the 1605 RO events on December 12, 2013 and the selected 200 RO events (blue triangle).

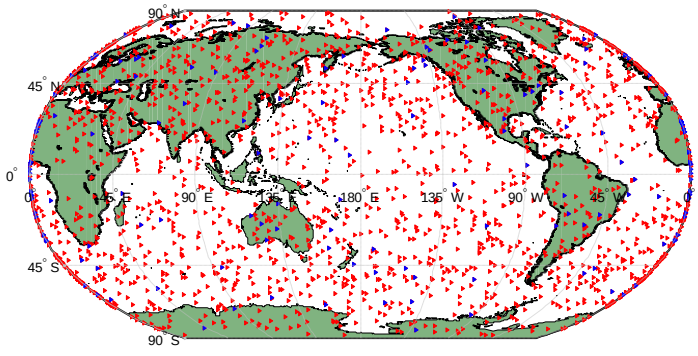

Fig.3. The global distribution of COSMIC RO events on December 12, 2013. Blue triangle represents the selected 200 RO events.

Atmos. Meas. Tech. Discuss., doi:10.5194/amt-2016-276, 2016
Manuscript under review for journal Atmos. Meas. Tech.
Published: 16 November 2016
© Author(s) 2016. CC-BY 3.0 License.

Atmospheric Measurement Techniques Discussions

252 There are 112 setting occultation events and 88 rising occultation events in the selected 200
253 occultation events. ROPP software is implemented to process the "atmPhs" profiles which are
254 collocated with the selected 200 RO events and derive profiles of refractivity and dry temperature,
255 which are denoted as R_phs and T_phs, respectively. We then respectively analyzed the setting
256 occultation events and rising occultation events to obtain the average relative deviation of
257 refractivity between R_N and R_phs, R_N and atmPrf, R_phs and "atmPrf".
258

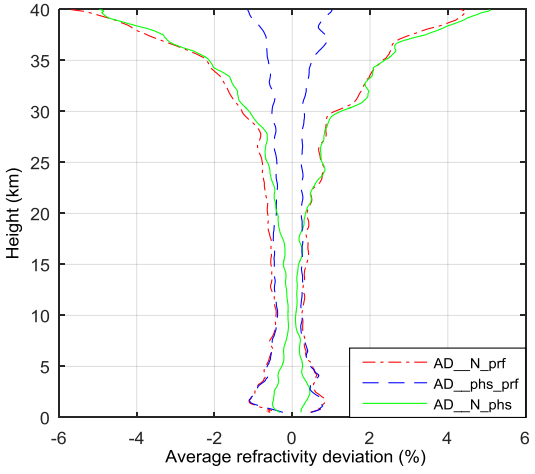

259

260 **Fig.4.** The statistical average relative deviation results of the refractivity for setting occultation events.
261 "AD_N_prf" denotes the average relatively deviation of refractivity between R_N and "atmPrf"; "AD_phs_prf"
262 expresses the average relatively deviation of refractivity between R_phs and "atmPrf"; "AD_N_phs" represents
263 average relatively deviation of refractivity between R_N and R_phs; "R_N" means the refractivity derived from
264 ND-derived AEP for the selected 200 RO events based on ROPP software; Ref_Phs means the refractivity
265 obtained from atmPhs profiles for the selected 200 RO events based on ROPP software.
266

Atmos. Meas. Tech. Discuss., doi:10.5194/amt-2016-276, 2016
Manuscript under review for journal Atmos. Meas. Tech.
Published: 16 November 2016
© Author(s) 2016. CC-BY 3.0 License.

Atmospheric Measurement Techniques Discussions

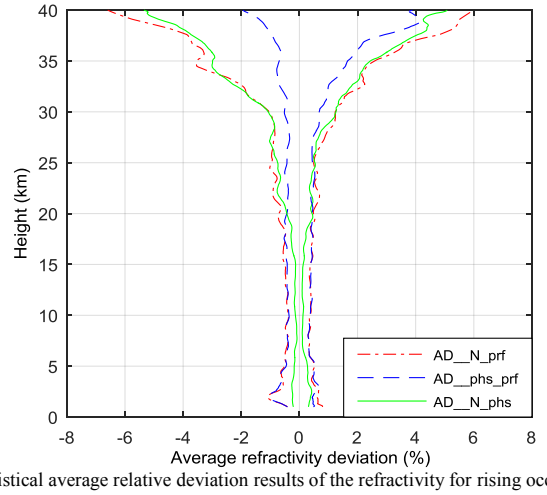

Fig.5. The statistical average relative deviation results of the refractivity for rising occultation events. "AD_N_prf" denotes the average relatively deviation of refractivity between R_N and "atmPrf"; "AD_phs_prf" expresses the average relatively deviation of refractivity between R_phs and "atmPrf"; "AD_N_phs" represents average relatively deviation of refractivity between R_N and R_phs; "R_N" means the refractivity derived from ND-derived AEP for the selected 200 RO events based on ROPP software; Ref_Phs means the refractivity obtained from atmPhs profiles for the selected 200 RO events based on ROPP software.

As it shows in Figure4 and Figure5, the blue dashed lines are all less than ±1.5% in setting occultation events and ±4.2% in rising occultation events, which once again verified the feasibility of ROPP software. In addition, Figure 4 and Figure 5 also indicate that the green lines are closer to 0 than the blue lines and red lines under the height of 20km, while the blue lines are closer to 0 than the red lines and green lines from the height of 20km to 40km. Besides, it is also obviously that the red lines and the green lines are gradually increases with height from 20km to 40km. At the same time, the statistics of the refractivity and dry temperature difference between ROPP-derived and "atmPrf" profiles for the selected 200 RO events are listed in Table 4.

Table 4. Summary of the comparison between ROPP-derived and "atmPrf". "ND-phs" repents the comparison between ND-derived and atmPhs-derived; "ND-prf" repents the comparison between ND-derived and "atmPrf"; "phs-prf" repents the comparison between atmPhs-derived and "atmPrf". (%)

Parameter	status	ND-phs	ND-prf	phs-prf
Refractivity	rising	1.64	1.91	0.93
	setting	1.52	1.63	0.51
Dry temperature	rising	2.49	3.21	1.65
	setting	2.35	2.42	0.72

Atmos. Meas. Tech. Discuss., doi:10.5194/amt-2016-276, 2016
Manuscript under review for journal Atmos. Meas. Tech.
Published: 16 November 2016
© Author(s) 2016. CC-BY 3.0 License.

Atmospheric Measurement Techniques Discussions

Table 4 provides the RMS of the comparison between ROPP-derived and "atmPrf" profiles in the rising and setting RO events, respectively. The statistical results indicate that the accuracy of setting RO events is better than the rising RO events. Besides, the RMS of average refractivity differences between ND-derived and atmPrf-derived is better than 2%, and the RMS of average dry temperature deviations between ND-derived and atmPrf -derived is better than 3.3%.

4.3 Comparison with ECMWF

CDAAC/UCAR center provides the ECMWF analyses produce, including "ecmPrf", "ecmPrf" and "eraPrf" profiles which collocated with radio occultation profiles. Among them, "ecmPrf" profiles contain temperature, pressure and moisture profiles generated from ECMWF analysis with 21 layers; "echPrf" files contain temperature, pressure and moisture profile from ECMWF high precision analysis field data with 88 layers; and "eraPrf" profiles include temperature, pressure and moisture profiles generated from the ERA interim model with 37 layers. Then, the observed COSMIC refractivity profiles utilizing ND method are compared with these three kinds of products, respectively. The mean relative refractivity deviation compared ND-derived and "atmPrf" profiles with ECMWF analyses are shown in Figure 6 with setting RO events and in Figure 7 with rising RO events.

Atmos. Meas. Tech. Discuss., doi:10.5194/amt-2016-276, 2016
Manuscript under review for journal Atmos. Meas. Tech.
Published: 16 November 2016
© Author(s) 2016. CC-BY 3.0 License.

Atmospheric Measurement Techniques Discussions

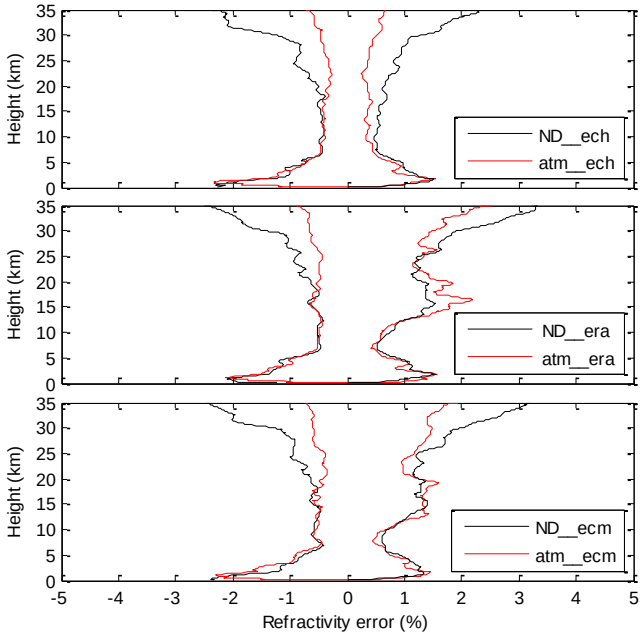

305

306 **Fig.6.** The mean relative refractivity deviation compared R_N and "atmPrf" with ECMWF analyses in setting RO
307 events. "ND__ech" represents the average relative refractivity deviation between ND-derived and "echPrf";
308 "atm__ech" denotes the average relative refractivity deviation between "atmPrf" and "echPrf"; "ND__era" shows
309 the average relative refractivity deviation between ND-derived and "eraPrf"; "atm__era" expresses the average
310 relative refractivity deviation between "atmPrf" and "eraPrf"; "ND__ecm" means the relative refractivity deviation
311 between ND-derived and "ecmPrf"; "atm__ecm" signifies the average relative refractivity deviation between
312 "atmPrf" and "ecmPrf"; "R_N" means the relative refractivity derived from ND-derived AEP for the selected 200
313 RO events based on ROPP software.

Atmos. Meas. Tech. Discuss., doi:10.5194/amt-2016-276, 2016
Manuscript under review for journal Atmos. Meas. Tech.
Published: 16 November 2016
© Author(s) 2016. CC-BY 3.0 License.

Atmospheric Measurement Techniques Discussions

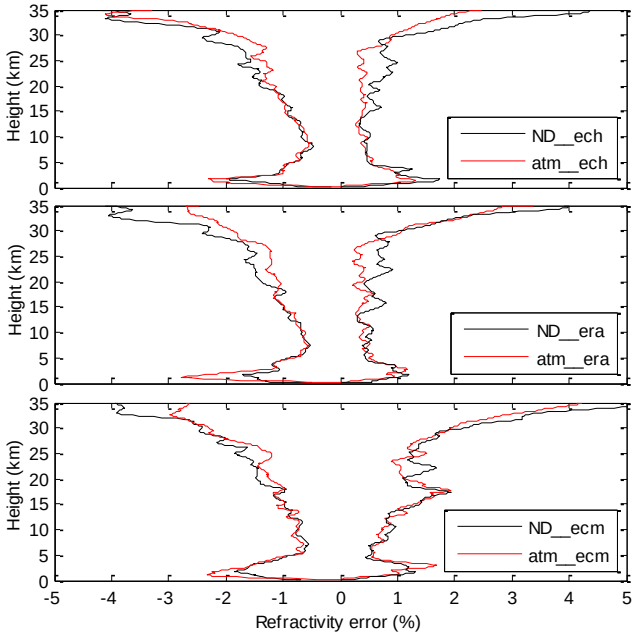

Fig.7. The mean relative refractivity deviation compared R_N and "atmPrf" with ECMWF analyses in rising RO events. "ND__ech" represents the average relative refractivity deviation between ND-derived and "echPrf"; "atm__ech" denotes the average relative refractivity deviation between "atmPrf" and "echPrf"; "ND__era" shows the average relative refractivity deviation between ND-derived and "eraPrf"; "atm__era" expresses the average relative refractivity deviation between "atmPrf" and "eraPrf"; "ND__ecm" means the average relative refractivity deviation between ND-derived and "ecmPrf"; "atm__ecm" signifies the average relative refractivity deviation between "atmPrf" and "ecmPrf"; "R_N" means the refractivity derived from ND-derived AEP for the selected 200 RO events based on ROPP software.

From Figure 6 and 7, it can be seen that the black lines are closer to 0 than the red lines below the height of 10km, while the red lines are closer to 0 than the black lines from the height of 10km to 35km. It may be due to the non-difference method cut down the noise level on the excess phase paths and thereby obtains less-biased refractivity with in regions of multipath signal propagation in the lower troposphere compared to single-difference technique. In addition, we also provide the statistics results between R_N and "atmPrf" and ECMWF analyses in Table 5.

Table 5. The summary of the mean relative refractivity deviation between COSMIC observations and ECMWF analyses. (%)

Parameter	status	ecmPrf	eraPrf	echPrf

Atmos. Meas. Tech. Discuss., doi:10.5194/amt-2016-276, 2016
Manuscript under review for journal Atmos. Meas. Tech.
Published: 16 November 2016
© Author(s) 2016. CC-BY 3.0 License.

Atmospheric Measurement Techniques Discussions

R_N	rising	1.82	1.46	1.49
	setting	1.32	1.34	1.06
atmPrf	rising	1.61	1.20	1.19
	setting	0.99	1.04	0.62

Table 5 presents that the accuracy of R_N is slightly worse than "atmPrf" compared to ECMWF analyses data. The mainly reason is subject to the effect of COSMIC receiver clock. Figure 8 shows the 5th and 6th COSMIC receiver clock error on December 12, 2013.

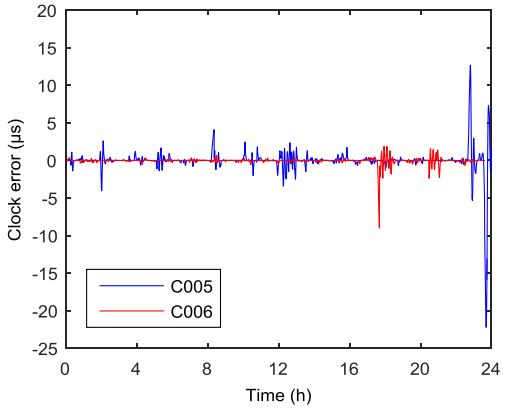

Fig. 8. The 5th and 6th COSMIC receiver clock error on December 12, 2013. "C005" represents the 5th COSMIC RO satellite; "C006" represents the 6th COSMIC RO satellite.

Figure 8 shows that both the 5th and 6th COSMIC satellite receiver clock offsets are very dramatic change, and it suggests that the COSMIC receiver without an ultra-stable oscillator. Moreover, it can be seen that the maximum clock difference between the neighboring two epochs is over 20 micro second from Figure 8. Therefore, it will bring in large noise when interpolating the COSMIC clock offset solutions into the temporal resolution of 20ms. Then, these noises will spread the excess Doppler and affect the accuracy of the refractive. In this study, the process of AEP for each COSMIC occultation event utilizing non-difference technique will be discarded when appearing a larger COSMIC clock oscillator with the same time of the RO event.

5 Conclusions

This study focused on the extraction of the AEP using the non-difference processing strategy. Firstly, the COSMIC POD processing is used to accurately determine the position and velocity of the center of mass of the satellite and the receiver offset based on PANDA software. Then,

Atmos. Meas. Tech. Discuss., doi:10.5194/amt-2016-276, 2016
Manuscript under review for journal Atmos. Meas. Tech.
Published: 16 November 2016
© Author(s) 2016. CC-BY 3.0 License.

Atmospheric Measurement Techniques Discussions

354 according to the UCAR/CDAAC provided "opnGps" profiles, taking the gravitational delay error,
355 the relativistic effects, the receiver clock error and the phase center offsets into account, the
356 atmospheric excess phases can be estimated with the help of precise Final GPS orbits and
357 transmitter clock offsets from GPS time using non-difference approach. Finally, the bending angle,
358 refractive and dry temperature profiles are performed from AEP using ROPP software. Next, the
359 refractivity profiles obtained from non-difference method are validated by using "atmPrf" profiles.
360 The case analyses of representative rising and setting occultation events indicate that the relative
361 refractive offset between ND-derived and "atmPrf" profile are better than ±2% below the height of
362 30km while the relative refractive offset gradually increases with the altitude from the height of
363 30km to 40km. In addition, the average relative refractive deviation of globally distributed 200
364 events between ND-derived and "atmPrf" profiles show that the comparison results are changing
365 from ±0.5% to ±6% in setting RO events, and from ±0.5% to ±7% in rising RO events. The
366 statistical results of refractivity and dry temperature are better than 2.0% and 3.3%, respectively.
367 Finally, the mean relative refractivity deviation between COSMIC observations and ECMWF
368 analyses present that non-difference approach reduces the noise level on the excess phase paths in
369 the lower troposphere compared to single-difference processing strategy. Subject to the impact of
370 receiver clock oscillation, the atmospheric excess phase process will fail using the non-difference
371 processing strategy in partial RO events. If the second-generation COSMIC receiver equipped an
372 ultra-stable oscillator, it would improve the quality of AEP using ND technique. Not only the
373 accuracy and the resolution of the results of the LEO POD, but also the accuracy of the refractive
374 can be improved in the future research.
375

376 **Refernece**s

377 Ashby, N.: Relativity in the global positioning system, Living Rev. Relativity., 6, 1, 2003..
378 http://www.livinggreviews.org/lrr-2003-1.
379 Beyerle, G., Schmidt, T., Michalak, G.: GPS radio occultation with GRACE: Atmospheric
380 profiling utilizing the zero difference technique, Geophysical Research Letters., 32, L1386,
381 2005.

© Author(s) 2016. CC-BY 3.0 License.

382 Bi, Y. M., Chen, J., Yang, G. L., Liao, M., Wu, R. H.: GPS occultation excess phase computed
383 utilizing the updated single difference technique, Acta Phys. Sin., 61(14), 149301, 2012.
384 CDAAC.: Algorithms for Inverting radio occultation signals in the neutral atmospheric research,
385 2005a. http://cosmic-io.cosmic.ucar.edu/caddc/doc/index.html.
386 CDAAC.: Algorithm description for LEO precision orbit determination with Bernese v5.0 at
387 CDAAC, COSMIC Project Office, University Corporation for Atmospheric Research., 2005b.
388 http://cosmic-io.cosmic.ucar.edu/caddc/doc/index.html.
389 COSMIC Operations Group.: CDAAC Data Products, 2013. http://cdaac-
390 www.cosmic.ucar.edu/cdaac/products.html.
391 Esteban, E., Vazquez, B., Borota, A., Grejner, B.: GPS-PWV estimation and validation with
392 radiosonde data and numerical weather prediction model in Antarctica, GPS Solut., 17, 29-
393 39, 2013.
394 Hajj G.A., Kursinski, E.R., Romans, L. J., Bertiger, W.I., Leroy, S.S.: A technical description of
395 atmospheric sounding by GPS occultation, J Atmos Sol Terr Phys. 64(4)., 451-469, 2002.
396 Hwang, C. W., Tseng, T. P., Lin, T. J.: Precise orbit determination for the FORMOSAT-
397 3/COSMIC satellite mission using GPS, Journal of Geodesy., 83, 477-489, 2009.
398 Kuo, B., Rocken, C., Anthes, R.: GPS radio occultation missions, The second Formosat3/
399 COSMIC Data Users Workshop, Boulder, Colorado., 2007.
400 Kursinski, E. R., Hajj, G. A., Schofield, J. T.: Observing earth's atmosphere with radio
401 Occultation measurements using the Global Positioning System, J. Geophs. Res., 102(D19),
402 23429-23465, 1997.
403 Liu, J.N., Zhao, Q.L., Ge, M.R.: Preliminary result of CHAMP orbit determination with PANDA
404 software, The International Symposium on GPS/GNSS. Sydney Australia., 2004.
405 Montenbruck, O., Garcia-Fernandez, M., Williams, J. Performance comparison of semi-codeless
406 GPS receivers for LEO satellites, GPS Solut., 10, 249-261, 2006. Doi:10.1007/s10291-006-
407 0025-9
408 Rocken, C., Anthes, R., Exner, M.: Analysis and Validation of GPS/MET Data in the neutral
409 atmosphere, Journal of Geophysical Research., 102(D25), 29849-29866, 1997.
410 Rocken, C., Kuo, Y. H., Schreiner, W.: COSMIC system description, special issue of terrestrial,

© Author(s) 2016. CC-BY 3.0 License.

411 atmospheric and oceanic science., 11(1), 21-52, 2000.

412 Rocken, C., Anthes, R., Exner, M., Hunt, D., Sokolovskiy, S., Ware, R.: Analysis and validation of
413 GPS/MET data in the neutral atmosphere, J Geophys Res., 102(D25), 29849-29866, 1997.

414 Wilson, J., Anderson, C., Baker, M.: Radiometric calibration of the advanced wind scatter meter
415 radar ASCAT carried onboard the METOP-A satellite, IEEE Transactions on Geoscience and
416 Remote Sensing, 48(8), 3236-3255, 2010.

417 Ware, R.: GPS Sounding of the atmosphere from low earth orbit: Preliminary results, Bull. Am.
418 Meteorol. Soc., 77, 19-40, 1996.

419 Wickert, J., Beyerle, G., Hajj, G., Schwieger, V., Reigber, C.: GPS radio occultation with
420 CHAMP: atmospheric profiling utilizing the space-based single difference technique, Geophys.
421 Res. Lett., 29, 1187, 2002.

422 Wickert, J., Reigber, C., Beyerle, G., Konig, R.: Atmosphere sounding by GPS radio occultation:
423 first results from CHAMP, Geophysical Research Letters., 28(17), 3263-3266, 2001.

424 Wickert, J.: GPS radio occultation with CHAMP and GRACE: A first look at a new and promising
425 satellite configuration for global atmospheric sounding, Ann. Geophys., 23, 653-658, 2005.

426 Wu, B. H., Fu, C. L., Liou, Y. A., Chen, W. J., Pan, H. P.: Quantitative analysis of the errors
427 associated with orbit uncertainty for FORMOSAT-3, In: Proceeding of the international
428 symposium on remote sensing (ISRS)., 87-90, 2005.

429 Schreiner, W., Rochen, C., Hunt, D.: Approach and quality assessment of single difference
430 processing of GPS radio occultation data at the UCAR CDAAC, A43A-0066, AGU Fall
431 Meeting, San Francisco, CA, December 11-15., 2005.

432 Schreiner, W., Rocken, C.: Quality assessment of COSMIC/FORMOSAT-3 GPS radio occultation
433 data derived from single-and double-difference atmospheric excess phase procession, GPS
434 Solut., 14, 13-22, 2010.

435 Schreiner, B.: COSMIC GPS POD and limb antenna test report. Internal report of UCAR, 2005.

436 Schreiner, W., Rochen, C., Hunt, D.: Approach and quality assessment of single difference
437 processing of GPS radio occultation data at the UCAR CDAAC, Eos Trans. AGU Fall
438 Meeting, San Francisco, Abstract A43a-0066., 2005.

439 Schreiner, W., Sokolovskiy, S., Hunt, D., Rocken, C., Kuo, Y. H.: Analysis of GPS radio

Atmos. Meas. Tech. Discuss., doi:10.5194/amt-2016-276, 2016
Manuscript under review for journal Atmos. Meas. Tech.
Published: 16 November 2016
© Author(s) 2016. CC-BY 3.0 License.

Atmospheric Measurement Techniques Discussions

occultation data from the FORMOSAT-3/COSMIC and Metop/GRAS missions at CDAAC, Atmos. Meas.Tech., 4, 2255-2272, 2011.

Senior, K., Ray, J., Beard, R.: Characterization of periodic variations in the GPS satellite clocks, GPS Solut., 12, 211-225., 2008. Doi:10.1007/s 10291-008-0089-9

Sokolovskiy, S., Hunt, D.: Statistical optimization approach for GPS/MET data inversions, presentation at URSI GPS/MET Workshop, Tucson, AZ., 1996.

Yen, N. L., Huang. Chen, J. F.: FORMOSAT-3/COSMIC GPS radio occultation mission: preliminary results, TEEE T. Geosci, Remote., 45, 3813-3825, 2007.

Yunck, T. P., Bertiger, W. I., Wu, S. C.: First assessment of GPS-based reduced dynamic orbit determination on TOPEX/POSEIDON, Geophysical Research Letter., 21 (7), 541-544, 1994.